Polymer Degradation and Stability 95 (2010) 1642–1654

Contents lists available at ScienceDirect

Polymer Degradation and Stability

journal homepage: www.elsevier.com/locate/polydegstab

Accelerated weathering of polyaramid and polybenzimidazole firefighter protective clothing fabrics

Rick Davis [a,*], Joannie Chin [b], Chiao-Chi Lin [b], Sylvain Petit [b]

[a] Building and Fire Research Laboratory, National Institute of Science and Technology, 100 Bureau Drive, MS-8665, Gaithersburg, MD 20899-8665, USA
[b] Building and Fire Research Laboratory, National Institute of Science and Technology, 100 Bureau Drive, MS-8615, Gaithersburg, MD 20899-8615, USA

ARTICLE INFO

Article history:
Received 17 February 2010
Received in revised form
19 May 2010
Accepted 20 May 2010
Available online 4 June 2010

Keywords:
Polyaramid
Polybenzimidazole
Firefighter
Accelerated weathering

ABSTRACT

Exposure to simulated ultraviolet sunlight at 50 °C and 50% relative humidity caused a significant deterioration in the mechanical performance of polyaramid and polyaramid/polybenzimidazole based outer shell fabrics used in firefighter jacket and pants. After 13 days of exposure to these conditions the tear resistance and tensile strength of both fabrics decreased by more than 40%. The polybenzimidazole containing fabric was less impacted by these conditions as it maintained approximately 20% more of its mechanical properties. These conditions also significantly degraded a water repellant coating on the fabric, which is critical to the water absorption performance of the outer shell fabrics. However, these conditions had little impact on the ultraviolet light protection of the outer shell as both fabrics still blocked 94% of ultraviolet light after 13 days of exposure. Confocal microscopy showed these conditions caused significant surface decomposition of and the switch from ductile to brittle failure of the polyaramid fibers. Cleavage of the amide linkages and the formation of oxidation species (as observed by Infrared spectroscopy) suggested these conditions caused photo-oxidation of the polyaramid fibers. There was little evidence of polybenzimidazole fiber degradation.

Published by Elsevier Ltd.

1. Introduction

Structural firefighter protective clothing is designed to shield the firefighter from environmental hazards, such as heat, abrasive surfaces, and some chemicals. The turnout gear (jacket and pants only) is typically a three layer system consisting of an outer shell (OS), moisture barrier (MB), and thermal liner (TL), as shown in Fig. 1 [1]. The inner-most layer often is the TL, which primarily provides thermal protection. This layer typically consists of a face-cloth, which slides easily along the skin to reduce the work required to move, and a spun-laced nonwoven insulating fabric. The air in the woven fabric provides thermal protection; therefore, the thicker the nonwoven fabric the better the thermal protection. However, a thicker TL is heavier and less breathable, and therefore less comfortable.

The middle layer is typically the MB, which often is a poly(tetrafluoroethylene) permeable film barrier laminated to a thin polyaramid woven or nonwoven backing substrate. The membrane limits the transport of some chemicals, pathogens, and water from the environment to the firefighter. The transport of any liquids across the MB toward the firefighter is a severe concern as it adds significant mass to the garment and deteriorates the TL performance, both of which can lead to severe injury and death from thermal exposure and heat stress. The backing substrate increases the durability of the TL. The nonwoven backing is less durable than the woven, but provides additional thermal protection.

The OS is the outermost layer and is the first line of defense against the abrasive and sharp physical hazards common to a fire scene. However, the OS also provides 25% to 30% of the turnout gear's thermal protection and serves to reduce water absorption. The OS is typically a woven fabric with a rip-stop construction being preferred as it prevents tear propagation. Similar to the TL, the OS is commonly constructed of polyaramid, polybenzimidazole, and/or poly(melamine-formaldehyde) fibers.

There are several publications describing the impact of simulated environmental conditions on fibers that are similar to those used in firefighter turnout gear [2–7]. Chin et al. [2] has shown that poly(p-phenylene-2,6-benzobisoxazole) fibers lost 30% tensile strength after a sequential exposure of 50 °C/60% relative humidity (RH) for 84 d and 60 °C/37% RH for 73 d. Attenuated Total Reflectance Infrared (ATR-IR) spectral analysis revealed with increasing exposure duration that there was an increase in benzoxazole ring cleavage (loss of 914 cm^{-1}, 1056 cm^{-1}, and 1362 cm^{-1} peak) and an increase in acid, alcohol, and amine group formation (1690 cm^{-1},

* Corresponding author. Tel.: +1 301 975 5901; fax: +1 301 975 4052.
E-mail address: rick.davis@nist.gov (R. Davis).

0141-3910/$ – see front matter Published by Elsevier Ltd.
doi:10.1016/j.polymdegradstab.2010.05.029

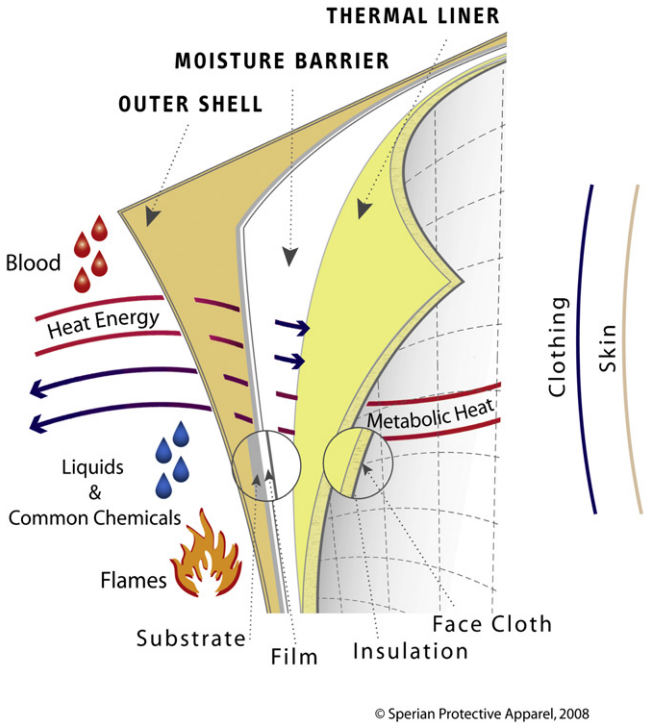

Fig. 1. Turnout gear schematic. Reproduced by the permission of SPERIAN Protective Apparel, Ltd [1].

3300 cm^{-1}). The impact of ultraviolet (UV) irradiation was not investigated.

Polybenzimidazole is a high performance polymer with exceptional thermal stability, and resistance to ignition, and hydrolysis [3,4]. While this polymer does have excellent chemical resistance, as compared to other high performance polymers, it has poor resistance to acids. However, as determined by Fourier Transform Infrared spectroscopy in a brine solution at 300 °C, the imidazole rings opened and cleaved to form hydrolysate derivatives, biphenyl tertra-amine, and benzodicarboxlyic acid [5].

Zhang et al. [6] reported the mechanical properties (tenacity, modulus, break extension and energy at break) for poly(*p*-phenylene terephthalamide) type fibers deteriorated linearly over the 145 h of the continuous UV irradiation at 40 °C ± 3 °C and 45% RH. The carbon arc lamp used in this study provided non-uniform light intensity across a portion of the UV spectrum (350 cm^{-1} to 420 cm^{-1} with intensity maximums at 360 cm^{-1}, 380 cm^{-1}, and 390 cm^{-1}). ATR-IR spectral analysis showed the UV irradiation caused a scission of the amide linkages in the polymer backbone resulting in the formation of carboxylic acid groups (1700 cm^{-1}), aldehydes (1716 cm^{-1}), and esters (1740 cm^{-1}). The authors' concluded that the UV irradiation caused photolytic degradation of the polymer, which was the reason for the drop in mechanical performance.

Tincher et al. [7] reported the mechanical properties (percent elongation and tenacity) of poly(*m*-phenylene isophthalate) type fibers deteriorated during the 100 h of the continuous UV irradiation (2500 watt carbon lamp) at 65 °C and 40% RH. For example, at 100 h the researchers measured only a 10% retained tenacity of the poly(*m*-phenylene isophthalate) fibers. By incorporating a three component stabilizer package into the poly(*m*-phenylene isophthalate) fibers, the UV degradation, and therefore, the mechanical property deterioration, was significantly mitigated. There was no analysis to measure the extent of polymer degradation.

Accelerated UV aging studies, such as those discussed above [6,7], commonly use carbon or xenon lamps. The exposure can be a single wavelength (usually 340 cm^{-1}) or broadband (usually 300 cm^{-1} to 400 cm^{-1}) with non-uniform intensities across a portion of the solar UV spectrum. The exposure dosage is generally reported on the intensity at a single wavelength (340 cm^{-1}). Zhang [6] and Tincher [7] did not report UV exposure dosage. However, using the information reported for the new Atlas Ci3000 Weather-Ometer as a guide, the acceleration was likely not greater than 2-suns [8]. In comparison, the simulated sunlight UV irradiance in our study presented here an approximate 17 sun acceleration across the entire solar UV spectrum (295 cm^{-1} to 495 cm^{-1})[9].

In the study presented here, we used an approach similar to the studies discussed above. More specifically, we exposed the fabrics of commercially available OS to simulated sunshine UV radiation at an elevated temperature and RH then measured the impact of the exposure on the mechanical performance and chemical composition of the fabrics. These woven fabrics were irradiated to UV (295 cm^{-1} to 495 cm^{-1}) at conditions similar to what is expected for firefighter protective clothing that is in-service (50 °C and 50% RH), and for a sufficient exposure duration to understand the impact these conditions will have over the typical service life (10 y) of turnout gear.

The performance of new fire fighting protective clothing and the guidelines for selecting, caring, and maintaining in-service protective clothing is defined in the United States by the National Fire Protection Association [10,11]. Recent amendments to these documents have indicated that UV exposure can damage the turnout gear; therefore, "do not store your gear in direct sunlight." The goal of this research was to determine the impact of UV irradiation (under typical in-service conditions) on fabrics commonly used in OS of commercial turnout gear and to determine to what extent the undergarments could be damaged from UV transmission through the OS.

2. Experimental[1]

2.1. Material description

Two commercially available OS commonly used in firefighter turnout ensembles were used for this study. KPB is a (40/60) number fraction % fiber blend and rip-stop weave fabric of polybenzimidazole and poly(*p*-phenylene terephthalamide) with a water repellant coating. NKB is a (93/5/2) number fraction % fiber blend and plain weave fabric of poly(*m*-phenylene isophthalate), poly(*p*-phenylene terephthalamide), and P-140 (antistatic fiber). This fabric has a different water repellant than the KPB fabric. Please refer to Table 1 for more information about these fabrics, Fig. 2 for pictures of these fabrics, and Fig. 3 for the chemical structure of the polymers.

Fabrics were delivered on manufacturer provided fabric rolls and stored as-received at ambient conditions (25 °C, ±5 °C and 20% ± 5% RH, (1σ)) in closed containers. The containers were not completely sealed, which allowed the fabrics to be conditioned to the room environment over the 10 months before testing. The room was kept dark when not in use; therefore, during storage and

[1] Certain commercial equipment, instruments or materials are identified in this paper in order to specify the experimental procedure adequately. Such identification is not intended to imply recommendation or endorsement by the National Institute of Standards and Technology, nor is it intended to imply that the materials or equipment identified are necessarily the best available for this purpose.

Table 1
Percent number of fiber type in the fabrics used in this study. Both fabrics were primarily polyaramid with KPB containing a significant portion of polybenzimidazole fibers. Both fabrics were finished with a fluoropolymer water repellant coating.

Fabric name	poly(*m*-phenylene isophthalate) (%)	poly(*p*-phenylene terephthalamide) (%)	polybenzimidazole (%)	Antistatic fiber (%)	Weight g/m^2 (oz/yd^2)	Fabric weave
NKB	93	5	–	2	254 (7.5)	Plain
KPB	–	60	40	–	254 (7.5)	Rip Stop

testing, the fabrics were exposed to very little of the low UV fluorescent lights in the storage room.

The UV irradiation was performed on fabrics cut into 10.2 cm × 7.6 cm (4 in × 3 in) swatches. From these swatches were cut 6.8 cm × 2.5 cm (2.66 in × 1.0 in) specimens for first measuring UV transmission, then for collecting FTIR spectra, and then for measuring the tear strength (Fig. 4). Following the tear strength experiments, the tensile strength was measured on the ply-twisted yarns from the non-torn, long edge of these tear strength specimens. After both mechanical performance experiments were complete, the surface morphology and fracture ends of the ply-twisted yarns were studied using a laser scanning confocal microscope. This same workflow was used for both the unexposed and the UV irradiated fabrics.

2.2. UV irradiation

High UV irradiance accelerated exposures of the fabrics were performed in the NIST 2 m integrating sphere-based weathering device, referred to as SPHERE (Simulated Photodegradation *via* High Energy Radiant Exposure). The mercury arc lamp system used with the SPHERE produced a collimated and highly uniform UV flux at each of the 32 testing ports (environmental chambers). A borosilicate glass window between the lamp system and the integrating sphere eliminated all UV wavelengths < 290 nm and a dichroic reflector in the lamps removed wavelengths > 450 nm. Additional details on the construction and properties of the SPHERE have been published elsewhere [12].

The conditions in the SPHERE environmental testing chambers was precisely controlled at 50 °C ± 0.1 °C and 50% ± 1% RH. Periodically a portion of the fabric was removed to perform the workflow analysis and tests discussed above. Due to experimental constraints, NKB and KPB fabrics were not always removed at exactly the same time for analysis and testing, but this difference in irradiation was small in comparison to the change in the measured properties. The total days on the SPHERE when a specimen was removed is reported in Table 2. The conversion of the d on the SPHERE to other parameters is also provided in this table and is discussed below.

The NIST SPHERE exposes specimens to the above described conditions for the entire 24 h of 1 d. The calculated daily UV irradiance dosage for these fabrics is 15.9 kJ/m^2 ± 0.02 kJ/m^2. Based on this daily dosage and the calculation of a representative daily natural dose (using data from the terrestrial tables in ASTM G173 [13]), 1 d on the SPHERE is equivalent to 7.4 d of Continuous Sun (CS).

Two parameters were calculated using these SPHERE (S) and Continuous Sun (CS) values. The Natural Conditions is a parameter that represents the number of days being simulated in the SPHERE when there is less than 24 h of sunlight in a day. The Natural Conditions (NC) value was calculated as

$$\mathrm{NC} = S \times 7.4(24\ \mathrm{h}/X) \quad (1)$$

where X is the duration of sunlight in a day (h), NC is the number of days the fabric is being exposed to X h of sunlight, S is the SPHERE exposure duration (d), and 7.4 is the CS conversion factor based on ASTM G173 (discussed above). Assuming in the real world there is 9 h of sun (X = 9 h) per d, then the NC conversion factor is 19.7 (7.4 × 24 h/9 h = 19.7). Therefore, in terms of UV irradiance dosage, 1 d on the SPEHRE (S = 1 d) is equivalent to 19.7 d (NC = 19.7) of natural conditions. This equation is provided in the first row of Table 2.

The other parameter calculated is the Turnout Gear Conditions (TGC), which represents how long the turnout gear is in service. TGC was calculated as follows

$$\mathrm{TGC} = S \times 7.4(24\ \mathrm{h}/Y) \quad (2)$$

where Y is the amount of time per d that the turnout gear is exposed to sunlight (h), TGC is the number of days the turnout gear is exposed to Y h of sunlight, and the other parameters are described above. Assuming that in 1 d of routine activities the turnout gear is exposed to the experimental conditions for 1 h (Y = 1 h), then the TGC conversion factor is 177.3 (7.4 × 24 h/1 h = 177.3). Therefore, in terms of UV irradiance dosage, 1 d on the SPHERE (S = 1 d) is equivalent to the turnout gearing being in service for 177.3 d. This equation is provided in the first row of Table 2.

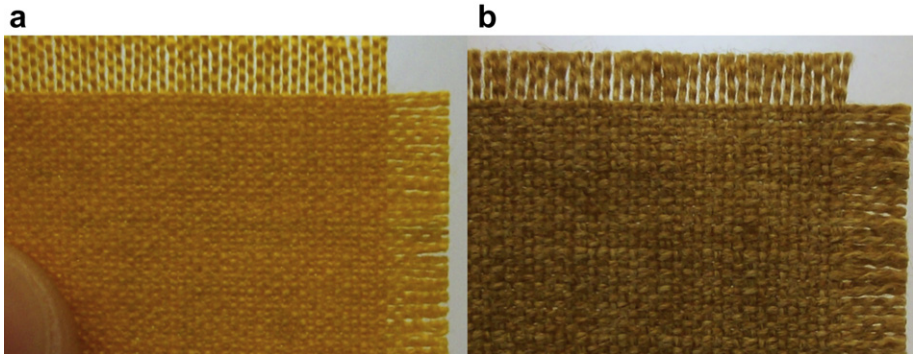

Fig. 2. Photographs of the (a) yellow NKB and the (b) gold/natural KPB fabrics. Note the different weave types and ply-twisted yarn density in the fill and warp direction.

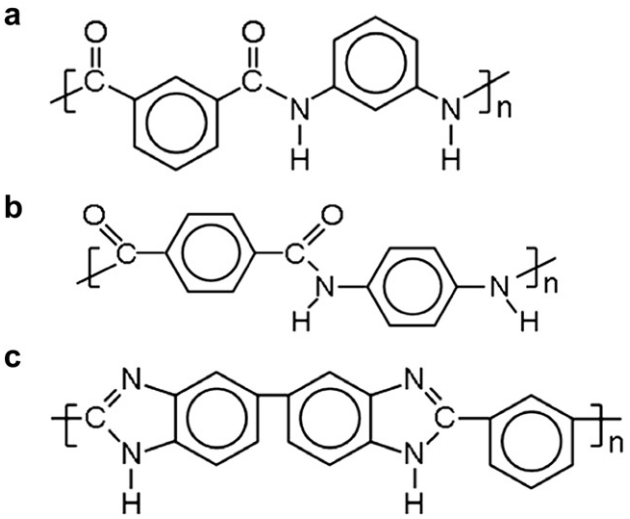

Fig. 3. Chemical structures of the polymer fibers. (a) poly(*m*-phenylene isophthalate), (b) poly(*p*-phenylene terephthalamide), and (c) polybenzimidazole.

2.3. Mechanical property testing

2.3.1. Tear strength

Tear strength experiments and data analysis were performed as described in ASTM D 2261-96 [14]. The experiments were conducted on an Instron model 5582 universal testing machine (Instron Corporation) equipped with custom grips as shown in Fig. 5(a). The tear strength specimens were 6.8 cm × 2.5 cm (2.66 in × 1.0 in) with a single 2.5 cm (1.0 inch) tear introduced at one end as shown in Fig. 4 (a). All testing was carried out in the same fabric direction; i.e., either parallel to the warp or weft direction [15]. The gauge length between grips was 2.5 cm, and crosshead speed was 50 mm/s. Four replicates of each fabric were tested per sampling interval.

2.3.2. Yarn tensile strength and % elongation (at break)

A TA Instruments RSA III Dynamic Mechanical-Thermal Analyzer (DMTA) (TA Instruments-Waters LLC, New Castle, DE) with transient capability was used to obtain the stress-strain properties of ply-twisted yarn extracted from the non-torn side of the tear testing specimens. The strain was calculated by the change in grips spacing as the instrument is not fitted with an extensometer. Therefore, the data is intended to represent trends and not absolute values.

As shown in Fig. 5(b), testing was carried out using fiber and film grips provided by the manufacturer. Specimen gauge length was 10 mm and specimen extension rate was 0.005 mm/s. A preload of 0.02 N ± 0.01 N was introduced to reduce slack in the ply-twisted yarn when it was secured on the fiber and film grips. However, this load wasn't always sufficient to remove the slack. Therefore, the remaining slack was removed from the data by linearly fitting the linear-elastic region of the stress-strain curves and shifting the curve to zero extension. The slack, and therefore the curve shift, is approximately 7% of the data. All tensile data in this manuscript is post fitting. A minimum of ten individual ply-twisted yarns were analyzed per sampling interval. The yarn diameter was measured using an optical microscope.

During the early methods development stage of this study, tensile strength of fabric strips was performed as described in ASTM D 5035-36. While the absolute values differed the trends were directly aligned with results obtained on yarn using the DMTA [16]. Due to material limitations, in this study, we measured the tensile strength on yarn rather than on fabric strips.

Table 2
Number of d the fabrics were irradiated with simulated sunshine UV radiation (SPHERE). SPHERE duration converted to the amount of time the fabrics were irradiated with an equivalent amount of UV solar radiation is CS, NC, and TGC, where CS is 24 h of solar radiation per d, NC is 9 h of solar radiation per d, and TGC is 1 h of solar radiation per d. TGC is the duration that turnout gear would be in service to receive the SPHERE equivalent radiation.

SPEHRE (d)	Continuous sun (d)	Natural conditions (d)	Turnout gear conditions	
			(d)	(y)
S	$CS = 7.4 \times S$	$NC = 19.7 \times S$	$TGC = 177.3 \times S$	
1	7.4	19.7	177.3	0.5
4	30	79	709	1.9
7	52	138	1241	3.4
13	96	256	2305	6.3
28	207	552	4964	13.6
42	311	827	7447	20.0
56	414	1103	9929	27.2
66	488	1300	11,702	32.0

2.4. Fabric analysis

2.4.1. Laser scanning confocal microscopy

Zeiss Model LSM510 and LSM510 META (*Carl Zeiss, Inc.*, Oberkochen, Germany) reflection Laser Scanning Confocal Microscopes (LSCM) with the same objectives were employed to qualitatively characterize the fiber surface and fracture end morphology of NKB and KPB. The incident laser wavelength was 543 nm for both of the two LSCMs. By adjusting the focal plane in the *z*-direction, a series of single images (optical slices) were stacked and digitally summed over the *z*-direction to obtain a 3-D image. The *z*-direction step size was 0.1 μm using objectives of 20×, 50×, and 150×. The pixel size of the LSCM images is 512 pixels by 512 pixels. At least two observations on three or more fiber samples were carried out per sampling interval. The manufacturer's software can be used to calculated surface roughness; however, our experience is the program works

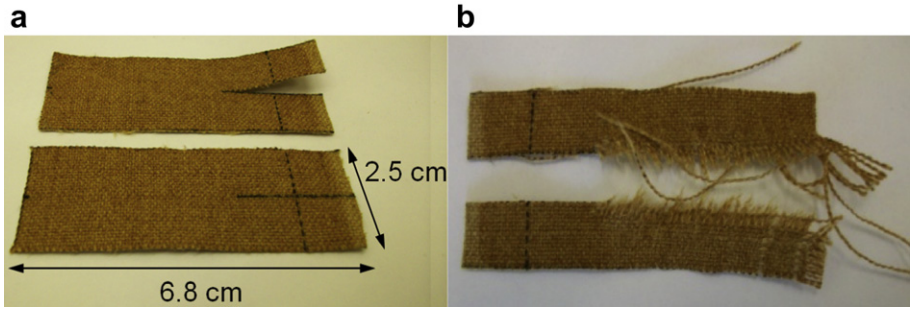

Fig. 4. Fabric swatch (a) before and (b) after tear strength experiment.

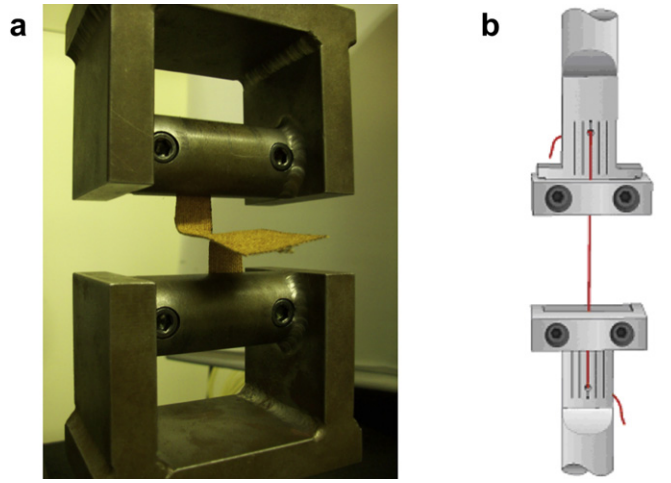

Fig. 5. Custom grips on Instron for tear strength (a) and tensile strength (b) experiments.

best on flat surfaces. Therefore, surface roughness calculations are approximations based on the size of pits and other surface deformations measured while collecting images.

2.4.2. Ultraviolet transmittance

Fig. 6a is a schematic of the UV transmittance measurement. The UV irradiation was provided by the NIST SPHERE with the irradiance as function of bandwidth that is provided in Fig. 6b and an output intensity of 480 W/m^2 [2,9]. UV–visible transmittance was measured using a Hewlett Packard 8452A diode array UV–Vis spectrophotometer (HP, Agilent) with a custom integrating sphere collector. UV spectra were recorded between 290 nm to 690 nm before (to record the dark current) and after the fabric specimen was mounted on black felt. At least three measurements were taken per sampling interval. The distance between the integrating sphere and the fabric specimen was a constant 2 cm for each measurement. Due to dark current drift, the calculated UV protection factor (UPF) and the average UV transmittance may be slightly shifted from the exact values.

2.4.3. Attenuated total reflectance fourier transform infrared (ATR-FTIR) spectroscopy

Infrared analysis was carried out using a Nicolet Nexus 670 FTIR (Nicolet Instrument Corporation) equipped with a mercury cadmium telluride (MCT) detector and a SensIR Durascope (Smiths Detection) attenuated total reflectance (ATR) accessory. Consistent pressure on the yarns was applied using the force monitor on the Durascope. Dry breathing quality air was used as the purge gas. FTIR spectra were collected at nine different locations on each 10.2 cm × 7.6 cm (4 in × 3 in) fabric swatch and were averaged over 128 scans. Spectral analysis, including spectral baseline correction and normalizing, was carried out using a custom software program developed in the Polymeric Materials Group at NIST to catalogue and analyze multiple spectra [9]. The spectra were baseline corrected and normalized using the peak at 781 cm^{-1} for NKB, and the peak at 820 cm^{-1} for KPB, both of which are attributed to out-of-plane aromatic C-H bending. Standard uncertainties associated with this measurement are ±1 cm^{-1} in wavenumber and ±5% in absorbance.

3. Results and discussion

3.1. Deterioration of tear and tensile strength

As described in ASTM D2261-96 [14], the fabric tear strength was calculated using the average of the five highest load points of

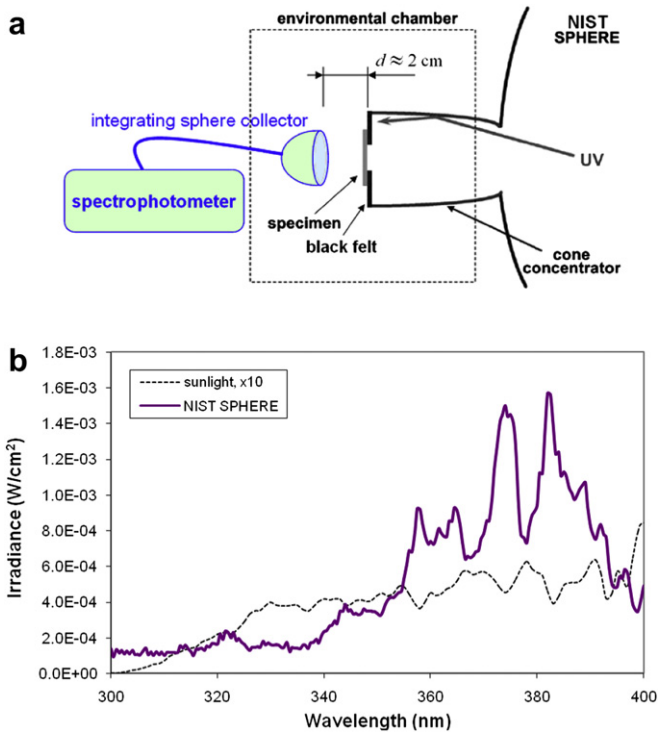

Fig. 6. (a) Schematic of UV transmittance measurement and (b) the Irradiance as a function of bandwidth for the NIST SPHERE and natural sunlight.

the load-extension curves. The tear strength as a function of exposure duration is reported in Fig. 7, Tables 3 and 4. NKB was exposed and analyzed first with the KPB studies following immediately afterwards. Based on the data collected from NKB, we reduced the exposure time and the testing frequency for KPB, which is the reason the exposure days in Table 3 are not exactly aligned with those in Table 4. Conversion of SPHERE (d) to NC (d) is described in Table 2.

For NKB, the largest deterioration of tear strength occurred after 1 d of UV irradiance (a 43% decrease to a value of 43 N ± 5.1 N) (Table 3). After another 2.6 d of irradiation, the tear strength dropped a total of 73% to a value of 20 N ± 1.1 N. The performance deterioration slowed down over the next 15.5 d with only an

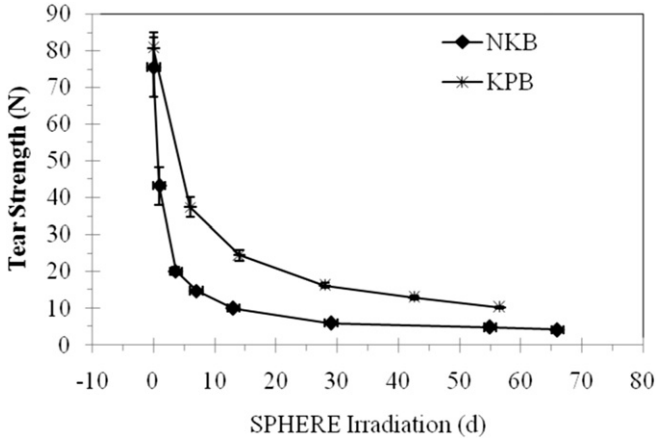

Fig. 7. Tear strength of fabrics as a function of SPHERE irradiation at 50 °C and 50% RH. As-received fabrics had similar tear strength, but the tear strength of the NKB deteriorated more rapidly under the exposure conditions. Errors bars represent a 2σ standard uncertainty.

Table 3
Tear strength of NKB fabric as a function of UV irradiation at 50 °C and 50% RH. 1 d of UV irradiation resulted in a 43% drop in tear strength. The deterioration rate decreased after 1 d of irradiation, but still dropped another 44% over the next 12 d of irradiation. Tear strength reported with 2σ uncertainty.

SPHERE (d)	NC (d)	Tear strength (N)	Tear strength decrease
0	0	75 ± 8.1	0%
0.9	18	43 ± 5.1	43%
3.6	71	20 ± 1.1	73%
7.0	139	15 ± 0.3	80%
13.0	257	10 ± 0.3	87%
29.0	574	5.9 ± 0.7	92%
55.0	1089	4.8 ± 0.6	94%
66.0	1307	4.1 ± 0.1	95%

average drop of 6.5% between (3.6 and 7) d, (7 and 13) d, and (13 and 29) d. By the time the deterioration reached a steady state at 29 d, the fabric had lost 92% of its original tear strength (to a value of 5.9 N ± 0.7 N) and lost only another 2% of its tear strength over the next 37 d of UV irradiation at 50 °C and 50% RH.

Within the experimental error, the tear strength of new KPB (81 N ± 4.3 N) is comparable to NKB (75 N ± 8.0 N). Similar to NKB, the tear strength of KPB deteriorated rapidly with a 54% decrease (to a value of 37 N ± 2.6 N) in 6 d of UV irradiation after which the deterioration slowed down with a 16% drop between (6 and 14) d, and another 10% drop between (14 and 28) d. Unlike NKB, the KPB tear strength deterioration did not reach a steady state, but rather a more semi-steady state as it continued to lose another 8% over the last 18 d of irradiation.

At any given irradiance day, the KPB had a tear strength that was on average 180% higher than the NKB, which is especially interesting because the tear strength of the new fabrics were statistically the same. This data suggests that KPB has superior resistance to these exposure conditions. For example, the tear strength at 56.6 d for KPB (10 N ± 0.2 N) is similar to the tear strength of NKB at 13 d (10 N ± 0.3 N).

The yarn tensile experiments were conducted on the DMTA using the UV irradiated and the unexposed NKB and KPB fabrics. The tensile strength and percent elongation values are shown Fig. 8, Tables 5 and 6. The slack correction (described in the experimental section) was applied to the data presented in these figures and tables. In calculating the stress, it was assumed that the cross section of the ply-twisted yarn was circular and the geometry was cylindrical. Though the tensile strength of the yarn was not the same as the tensile strength measured on pieces of fabric, experiments conducted at the onset of this study showed the trends were well aligned [16].

The unexposed NKB has a 55 MPa ± 7.9 MPa tensile strength, and 41% ± 4% elongation (Fig. 8 and Table 5). Similar to the deterioration in tear strength, the tensile properties also deteriorated rapidly with a 40% and 54% decrease in the tensile strength and percent elongation, respectively, after 1 d of UV irradiation at 50 °C and 50% RH. The tensile strength continued to follow a very similar deterioration profile as discussed above for the tear strength with another drastic drop in performance (27% decrease to a value of 18 MPa ± 2 MPa) over the next 2.6 d, followed by a slower performance deterioration over the next 24.4 d (29% decrease to a value of 3 MPa ± 0.9 MPa) and then reaching a steady state tensile strength of 1.3 MPa ± 0.3 MPa (98% total decrease) for the reminder of irradiation. The decrease in percent elongation is more severe than the tear and tensile strength as it decreased an additional 31% between (0.9 and 3.6) d, then reached a steady state for the remainder of the exposure time with a final percent elongation of 6% ± 1.8% (85% decrease).

Table 4
Tear strength as a function of UV irradiation at 50 °C and 50% RH for KPB. Similar to NKB, the deterioration rate was higher at the onset of irradiation. KPB tear strength was less impacted by irradiation as evidenced by the 70% decrease at 14 d, as compared to 87% at 13 d for NKB. Tear strength reported with 2σ uncertainty.

SPHERE (d)	NC (d)	Tear strength (N)	Tear strength decrease
0	0	81 ± 4.3	0%
6	119	37 ± 2.6	54%
14	277	24 ± 1.5	70%
28	554	16 ± 0.7	80%
42.6	843	13 ± 0.5	84%
56.6	1121	10 ± 0.2	88%

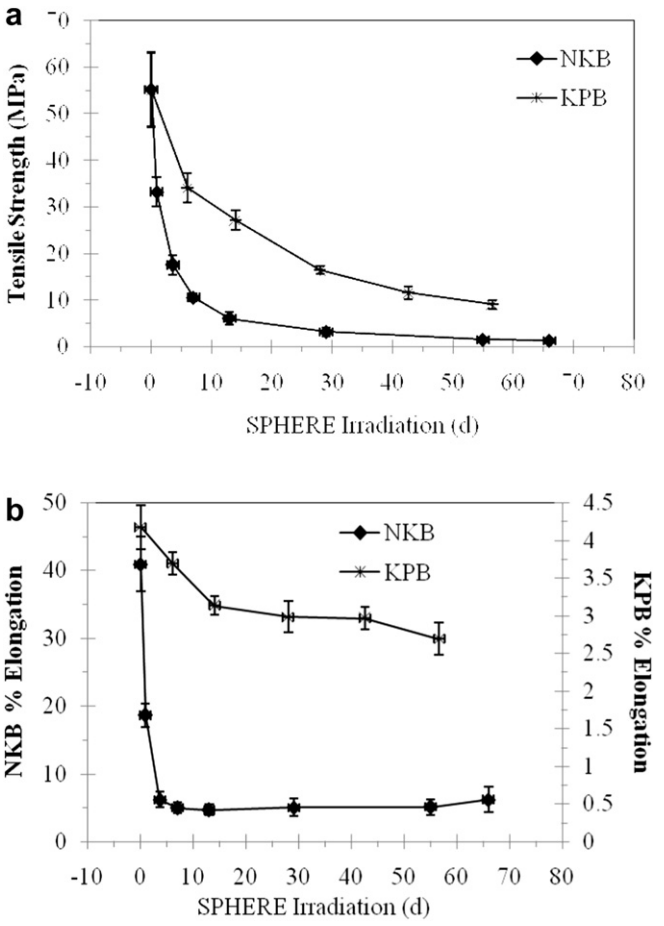

Fig. 8. (a) Tensile strength and (b) % elongation of fabrics as a function of UV irradiation at 50 °C and 50% RH. The largest decrease in tensile properties occurred after the initial UV irradiation. Unexposed NKB and KPB fabrics had similar performance; however, KPB maintained more of its tensile strength over the 55 d of irradiation. Errors bars represent a 2σ standard uncertainty.

The tensile strength performance for NBK and KPB is very similar to the measured tear strength deterioration discussed above. The KPB has superior resistance to the exposure conditions as evidenced by KPB having a less severe tensile strength deterioration rate and higher tensile strength after irradiation (Fig. 8, Tables 5 and 6). More specifically, the tensile strength for unexposed NKB (55 MPa ± 8.0 MPa) and unexposed KPB (55 MPa ± 5.3 MPa) are the same within the uncertainty of the measurement. However, a tensile strength of 11 MPa ± 0.9 MPa was measured at 7 d for NKB, but a value of 10 MPa is calculated not to occur until 50 d of irradiation for KPB.

A similar trend in deterioration of percent elongation was also measured for KPB (Fig. 8, Tables 5 and 6). While the percent

Table 5
Tensile strength and % elongation as a function of UV irradiation at 50 °C and 50% RH for NKB. Tear strength reported with 2σ uncertainty.

SPHERE (d)	NC (d)	Tensile strength (MPa)	Tensile strength decrease	%-Elongation	%Elongation decrease
0	0	55 ± 7.9	0%	41 ± 4.1	0%
0.9	18	33 ± 3.1	40%	19 ± 1.7	54%
3.6	71	18 ± 2.1	67%	6 ± 1.2	85%
7.0	139	11 ± 0.9	80%	5 ± 0.8	88%
13.0	257	6 ± 1.4	89%	5 ± 0.8	88%
29.0	574	3 ± 0.9	95%	5 ± 1.4	88%
55.0	1089	1.5 ± 0.4	97%	5 ± 1.1	88%
66.0	1307	1.3 ± 0.3	98%	6 ± 1.8	85%

elongation for the unexposed KPB ($4\% \pm 0.3\%$) is an order of magnitude lower than the unexposed NKB ($41\% \pm 4\%$), the percent elongation for these two fabrics are significantly closer after 7 d of exposure with values in the range of 3% to 6%.

The KPB fabrics maintain more of its mechanical properties after exposure. However, since we cannot delineate polymer type and construction contributions to the tear strength, tensile strength, and percent elongation performance of these fabrics (Table 1), we cannot explain if the mechanical performance deterioration rate of the fabrics as a function of irradiation is a result of the polymer type, construction, or both.

3.2. Low UV transmittance

The use of factors, such as the UV protection factor (UPF) and the average UV transmittance, aids in quantifying the UV protection properties of garments [17–19], such as the OS of firefighter protective clothing. As the UV transmission through the OS increases (UPF decreases) there is an increasing potential for UV radiation damage to the underlying layers (MB and TL) of the protective gear.

According to the American Association of Textile Chemists and Colorists (AATCC) test method 183-2000 [17], UPF is calculated as "the ratio of the erythemally weighted ultraviolet radiation (UVR) irradiance at the detector with no specimen to the erythemally weighted UVR irradiance at the detector with a specimen (fabric) present". The UPF calculation is

$$\mathrm{UPF} = \frac{\sum_{280\ \mathrm{nm}}^{400\ \mathrm{nm}} E_\lambda \times S_\lambda \times \Delta\lambda}{\sum_{280\ \mathrm{nm}}^{400\ \mathrm{nm}} E_\lambda \times S_\lambda \times T_\lambda \times \Delta\lambda} \tag{3}$$

where E_λ is relative erythemal effectiveness function, S_λ is solar spectral irradiance ($W/(cm^2 \times nm)$) T_λ is the measured spectral transmittance of the fabric (%), $\Delta\lambda$ is the measured wavelength interval (nm). The E_λ *and* S_λ functions describe the relative sensitivity of erythema (skin redness) to individual wavelengths and the spectral distribution of sunlight as it reaches the earth's surface. The average A-range UV transmittance was calculated by

$$T_{(\mathrm{UV\text{-}A})^{av}} = \frac{\sum_{315\ \mathrm{nm}}^{400\ \mathrm{nm}} T_\lambda \times \Delta\lambda}{\sum_{315\ \mathrm{nm}}^{400\ \mathrm{nm}} \Delta\lambda} \tag{4}$$

and the average B-range UV transmittance was calculated by

$$T_{(\mathrm{UV\text{-}B})^{av}} = \frac{\sum_{280\ \mathrm{nm}}^{315\ \mathrm{nm}} T_\lambda \times \Delta\lambda}{\sum_{280\ \mathrm{nm}}^{315\ \mathrm{nm}} \Delta\lambda} \tag{5}$$

According to ASTM D6603-00 [20], the rating categories of UV protections are "good", "very good" and "excellent", for UPF values of 15 to 24, 25 to 39, and greater than 40, respectively. The UPF protection values (rating) for the unexposed NKB is 43 ± 0.6 ("excellent") and 25 ± 0.3 ("very good") for the unexposed KPB (Tables 7 and 8) [20]. After 13 d of UV irradiation at 50 °C and 50% RH, the UPF deteriorated by 42% to a value of 25 ± 0.3 for the NKB, which is the same UPF value for the unexposed KPB. The UPF value for NKB decreases an additional 4% over the next 16 d of exposure then reaches a steady state value of 18 ± 0.3 for the remaining 27 d of the study. Even though the UPF value for the NKB decreased by 66% after 66 d of irradiation, the fabric still had a "good" UPF rating.

The unexposed KPB fabric started with a borderline "good/very good" rating and after 56.6 d of irradiation still had a "good" rating (28% deterioration from a UPF value of 25 ± 0.3 to 18 ± 0.3). Compared to NKB, KPB had a lower UPF value when the fabrics were new (unexposed), but after 14 d of irradiation these fabrics had indistinguishable UV blocking performance.

Even though the fabrics have experienced significant chemical (discussed below) and mechanical decomposition (discussed above) as a result UV irradiation, the fabrics maintained a high level of UV blocking performance. A UPF value of 18 ± 0.3 indicates only $1/18^{th}$ of the sun's UV radiation passes through the fabric, which is still sufficient for a "UV protection" rating. Even at this lowest level of UPF protection (18 ± 0.3) provided by these fabrics, the undergarments (MB and TL) will not be exposed to sufficient solar UV radiation for photolytic degradation of these undergarments to be a concern.

Table 6
Tensile strength and % elongation as a function of UV irradiation at 50 °C and 50% RH for KPB. Tear strength reported with 2σ uncertainty.

SPHERE (d)	NC (d)	Tensile strength (MPa)	Tensile strength decrease	%-Elongation	%Elongation decrease
0	0	55 ± 5.3	0%	4 ± 0.3	0%
6	119	34 ± 5.6	38%	4 ± 0.2	0%
14	277	27 ± 3.2	51%	3 ± 0.1	25%
28	554	16 ± 2.2	71%	3 ± 0.2	25%
42.6	843	12 ± 2.4	78%	3 ± 0.1	25%
56.6	1121	9 ± 1.5	84%	3 ± 0.2	25%

Table 7
Ultraviolet protection factor (UPF) and the average UV transmittance of NKB as a function of UV irradiation. The UPF value decreased 54% after 29 d of irradiation. However, the NKB fabric still blocked 94.5% of the UV radiation. The UPF standard uncertainty was ±5% of the value (2σ).

SPHERE (d)	UPF	$T_{(280-400)}$ (%)	$T_{(280-315)}$ (%)	$T_{(315-400)}$ (%)	$T_{(400-500)}$ (%)
0.0	43	0.12	0.00	0.17	0.10
13.0	25	0.18	0.00	0.26	0.41
29.0	18	0.18	0.00	0.26	0.57
55.0	18	0.23	0.00	0.33	0.56
66.0	18	0.24	0.00	0.34	0.54

3.3. Fiber surface degradation

LSCM was used to visually observe the fiber morphology and fracture ends (Figs. 9–14). LSCM images of the poly(*m*-phenylene isophthalate) fibers from NKB are shown in Figs. 9 and 10. LSCM images of KPB are shown in Figs. 11–14, where Figs. 11 and 12 are the poly(*p*-phenylene terephthalamide) brown fibers and Figs. 13 and 14 are the polybenzimidazole yellow fibers. While color was the primary mechanism for delineating the poly(*p*-phenylene terephthalamide) brown from the polybenzimidazole yellow fibers, FTIR spectroscopy was frequently used for confirmation.

The poly(*m*-phenylene isophthalate) fibers from NKB were visually inspected under the LSCM at (0, 13, and 66) d of SPHERE irradiation before and following tensile testing (Figs. 9 and 10, respectively). After 13 d of UV irradiation at 50 °C and 50% RH, the surface of the fiber was rough with an estimated 10% surface pitting. At 66 d of irradiation, there was an estimated 25% surface pitting and the surface was significantly rougher with a multitude of intersecting surface channels. These observations are classical identifiers of chemical and/or mechanical property decomposition [21].

Evidence of chemical and property decomposition initiated by UV irradiation was supported by the LSCM images of the fracture ends and surface of the poly(*m*-phenylene isophthalate) fiber following the tensile experiments. The unexposed poly(*m*-phenylene isophthalate) fiber maintained its cylindrical shape and a regular patterned finish (possible surface delamination) was observed that is frequently associated with ductile failure at break (Fig. 10a) [21]. The "necking" at the fracture end was another indicator of ductile failure of this unexposed fiber. At 13 d of irradiation, the failure mechanism had switched from ductile to brittle failure as evidenced by the sharp cleavage and granulated fracture end of the fiber (Fig. 10b). In addition to the rough and pitted surface, there was no regular patterned finish and the fiber was slightly deformed. At 66 d of irradiation, the shape deformation was significant as the fiber appears to be deformed into a more oval shaped cylinder. These observations from the LCSM images are consistent with the measured mechanical property deterioration of the NKB fabric.

The poly(*p*-phenylene terephthalamide) fibers from KPB were visually inspected under the LSCM at (0, 14, and 56.6) d of SPEHRE irradiation before and following tensile testing (Figs. 11 and 12, respectively). The UV irradiation had a similar impact on the poly (*p*-phenylene terephthalamide) fibers as discussed previously for the poly(*m*-phenylene isophthalate) fibers, except the surface deterioration was significantly more severe in the poly(*p*-phenylene terephthalamide) fibers, 60% surface pitting at 66 d of irradiation. However, these fibers still maintained some level of ductility as evidenced by the splitting and fibrillation at the fracture ends, but deterioration was still occurring as the ends are becoming more granular with increasing irradiation time. Similar to poly(*m*-phenylene isophthalate) fibers, these exposed poly(*p*-phenylene terephthalamide) fibers were also deformed.

Table 8
Ultraviolet protection factor (UPF) and the average UV transmittance of KPB as a function of UV irradiance. Similar to NKB the UPF value was 18 ± 0.3 at 28 d of irradiation and blocked 94.5% of the UV radiation. The UPF standard uncertainty was ±5% of the value (2σ).

SPHERE (d)	UPF	$T_{(280-400)}$ (%)	$T_{(280-315)}$ (%)	$T_{(315-400)}$ (%)	$T_{(400-500)}$ (%)
0.0	25	0.12	0.10	0.12	0.22
14.0	18	0.08	0.05	0.10	0.17
28.0	18	0.08	0.03	0.11	0.14
42.6	18	0.11	0.04	0.14	0.20
56.6	18	0.17	0.36	0.09	0.14

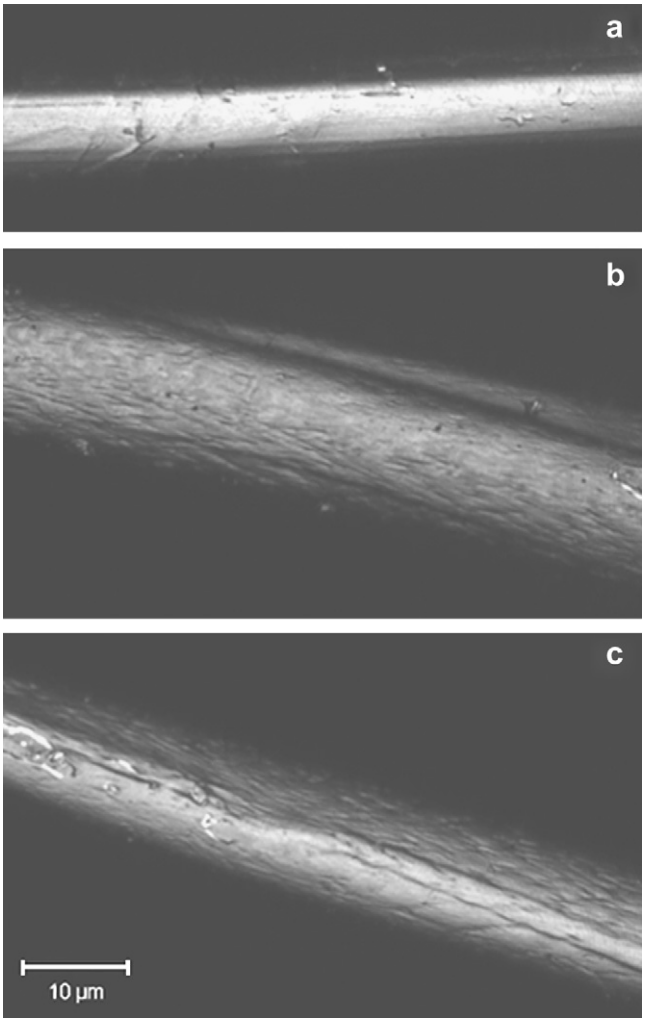

Fig. 9. Confocal microscope images of poly(*m*-phenylene isophthalate) fibers from NKB following (a) 0 d, (b) 13 d, and (c) 66 d of UV irradiation at 50 °C and 50% RH. The UV radiation caused surface pitting and deformed the fiber shape, both of which are consistent with polymer degradation and a loss of mechanical properties.

The polybenzimidazole fibers from KPB were visually inspected under the LSCM at (0, 14, and 56.6) d of irradiation before and after tensile testing (Figs. 13 and 14, respectively). The UV irradiation had a similar impact on the polybenzimidazole fibers as discussed for the poly(*m*-phenylene isophthalate) fibers, except the fracture end morphology (sharp cleavage) was independent of exposure duration and the surface pitting was less severe (12% at 55.6 d of irradiation).

As indicated earlier, the difference in mechanical performance deterioration rate as a function of irradiation time is difficult to explain because the polymer type and construction of these fabrics are different. The LCSM images of the polyaramid fibers showed

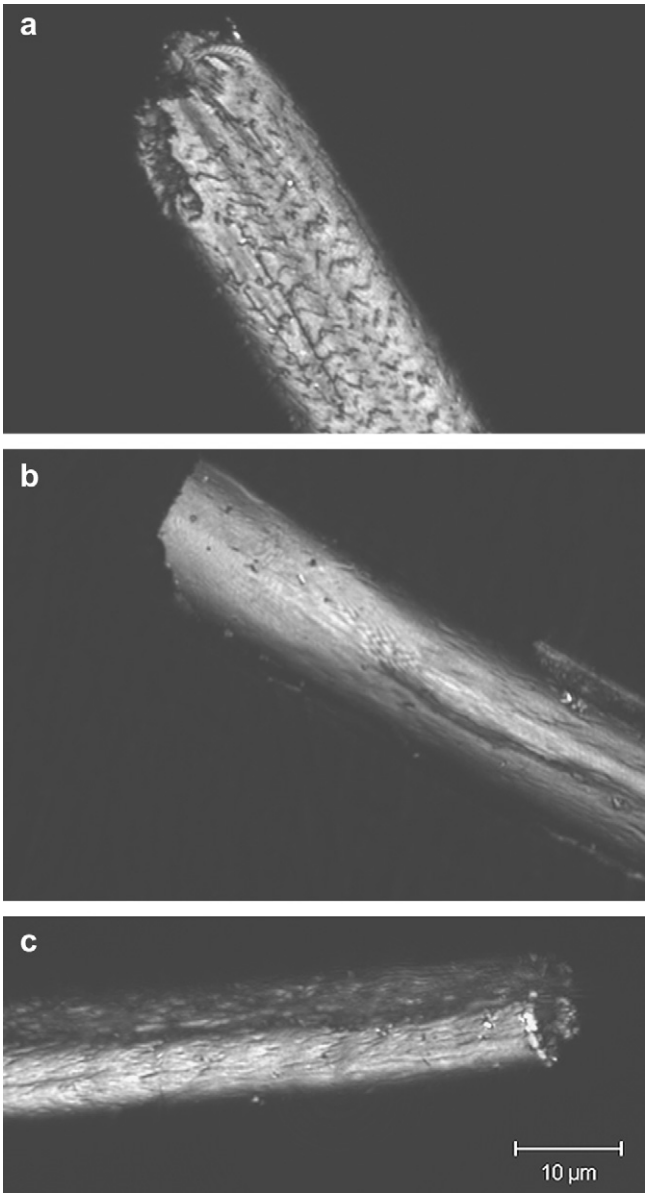

Fig. 10. Confocal microscope images of poly(*m*-phenylene isophthalate) fiber fracture ends following tensile failure. These fibers are from NKB fabric following (a) 0 d, (b) 13 d, and (c) 66 d of UV irradation at 50 °C and 50% RH. The UV radiation resulted in a change from ductile failure (necking of fiber end) to brittle failure (sharp cleavage in b and c), which is consistent with a loss of mechanical properties.

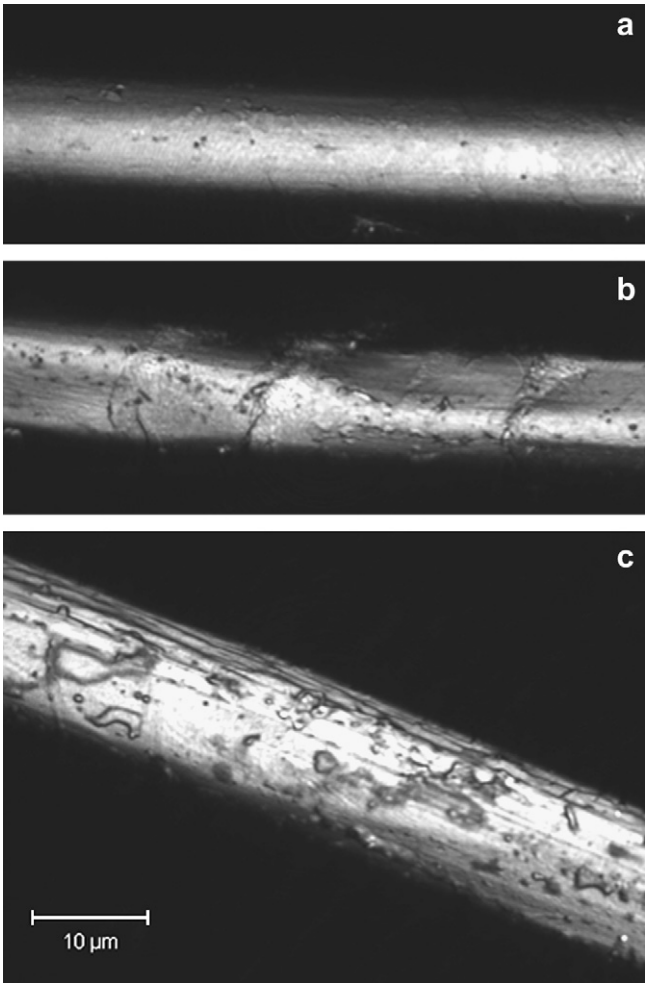

Fig. 11. Confocal microscope images of poly(*p*-phenylene terephthalamide) fibers from KPB following (a) 0 d, (b) 14 d, and (c) 56.6 d of UV exposure at 50 °C and 50% RH. The UV radiation caused severe surface pitting and shape deformation, both of which are consistent with polymer degradation and a loss of mechanical properties.

significant visual evidence of decomposition, where as the polybenzimidazole fibers appeared to be only slightly physically affected by the irradiation. Therefore, we assume the polybenzimidazole fibers in the KPB fabric maintained its properties after irradiation.

3.4. Polymer decomposition (photo-oxidation)

ATR-FTIR analysis was used to elucidate the chemical changes induced by the UV irradiation. Interpretation of FTIR spectra was based on the literature peak assignments of poly(*m*-phenylene isophthalate), poly(*p*-phenylene terephthalamide), and polybenzimidazole that are provided in Tables 9–11 [22–29]. The FTIR spectra of KPB and NKB fabrics are provided in Fig. 15. The change in peak intensity and, therefore, the change in concentration of species in the irradiated fabrics are believed to be a result of photo-oxidation of the polymers. The suggested degradation products are based on those reported in the above mentioned publications, where these species were identified by FTIR analysis of model compounds.

Both fabrics were treated with a proprietary polymeric water repellant coating. The purpose of the coating was to enable the OS to pass the water absorption requirements defined in NFPA 1971. Since the polymer fibers all contained sp^2 hybridization C–H bonding, the peaks at 2880 cm^{-1} and 2930 cm^{-1} were due to sp^3 hybridization C–H bonding, and the water repellant coating contains sp^3 C–H bonding, we assigned these two peaks to this water repellant coating (Fig. 15). After 13 d of UV irradiation these peaks have significantly diminished, which suggests the coating was degrading. These peaks were gone, and therefore so was the coating, after 13 d of UV irradiation of the KPB fabric, and 55 d of UV irradiation of the NKB fabric. These fabrics have different water repellant coatings. Therefore, these spectra indicate the coating on the NKB fabric has superior UV resistance. Depending on the magnitude of the coating's contribution to the OS performance, after 13 d of UV irradiation the OS may have degraded sufficiently to be in danger of not complying with the water absorption requirements defined in this NFPA regulation.

A few of the key IR peaks for these polyaramids are the N–H trans-amide stretching at 3320 cm^{-1}, the Amide I at 1650 cm^{-1}, the

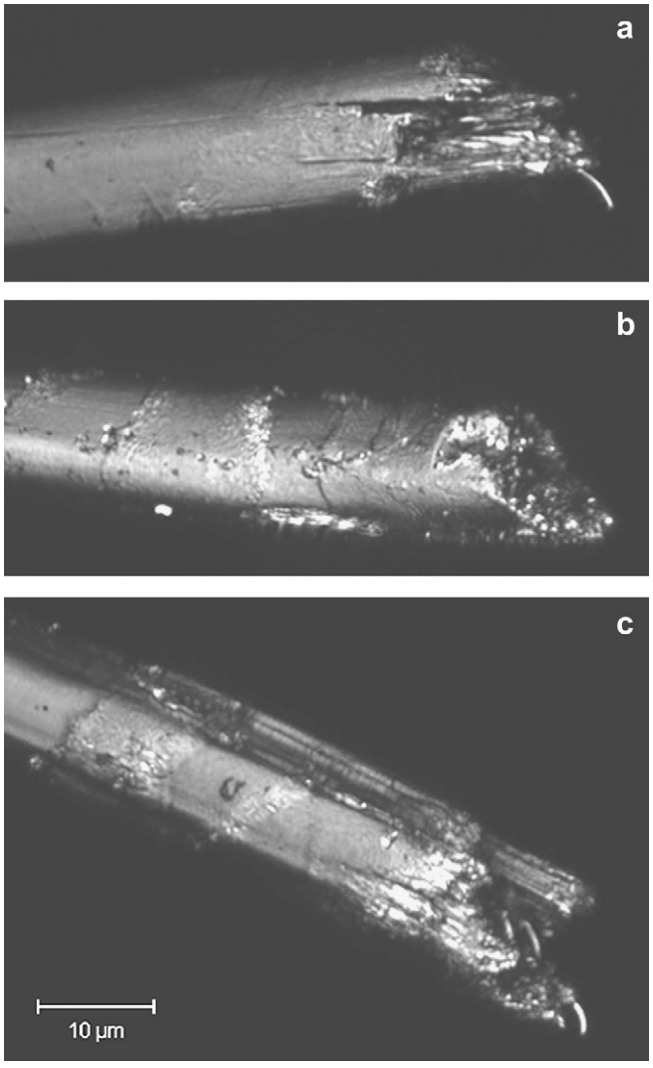

Fig. 12. Confocal microscope images of poly(*p*-phenylene terephthalamide) fiber fracture ends following tensile failure. These fibers are from KPB fabric following (a) 0 d, (b) 14 d, and (c) 56.6 d of UV irradiation at 50 °C and 50% RH. The UV radiation resulted in a change from ductile failure (necking of fiber end) to brittle failure (sharp cleavage in b and c), which is consistent with a loss of mechanical properties.

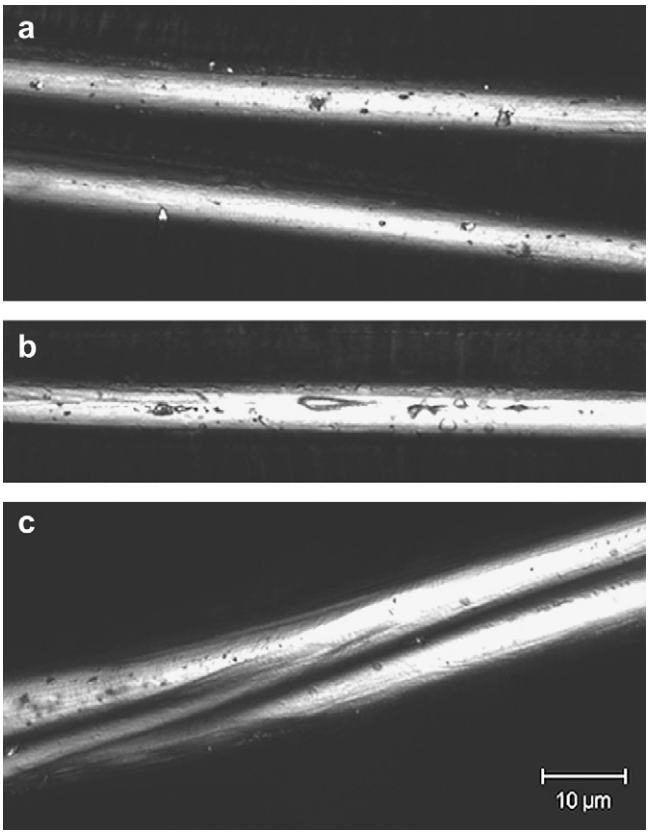

Fig. 13. Confocal microscope images of polybenzimidazole fibers from KPB following (a) 0 d, (b) 14 d, and (c) 56.6 d of UV irradiation at 50 °C and 50% RH. The UV radiation caused surface pitting and deformed the fiber shape, both of which are consistent with polymer degradation and a loss of mechanical properties.

aromatic ring C═C stretching at 1600 cm^{-1}, the Amide II at 1536 cm^{-1}, and the aromatic C–N stretching at 1300 cm^{-1} (Fig. 15 and Tables 9–11). Most of the polyaramid peaks exist in both the NKB and KPB fabrics; however, only the NKB spectrum is labeled to avoid cluttering the spectra. Only the 1600 cm^{-1} polyaramid peak for the KPB fabric was not observed because in poly(*p*-phenylene terephthalamide) it is a low absorbing shoulder, rather than a strong absorbing peak, as seen for poly(*m*-phenylene isophthalate), and this shoulder is convoluted with a peak for polybenzimidazole.

For the KPB fabrics, the polybenzimidazole peaks were difficult to identify as these were not well resolved from the poly(*p*-phenylene terephthalamide) peaks. The main IR peaks that were visible for the polybenzimidazole fibers were the aromatic N–H stretching at 3050 cm^{-1}, the C═C/C═N stretching at 1626 cm^{-1}, and the benzene ring vibrations at 1050 cm^{-1} (Fig. 15). The low absorbance of these peaks suggests that the polybenzimidazole is a minor component of the KPB fabric.

After UV irradiation, new peaks appeared presumably due to the formation of acids, alcohols, and/or amines (broad peak or overlapping of broad peaks centered at 3200 cm^{-1} for O–H and N–H stretching) and the formation of acids (C═O stretching at 1720 cm^{-1}). This observation, along with the intensity reduction of the Amide II (1536 cm^{-1}) and Amide I (1650 cm^{-1}) peaks, indicates these conditions resulted in a cleaved of the amide bonds (C–N) in the polymer backbone and the formation of carboxylic acids as well as other oxidized species, presumably by photo-oxidation. The intensity of the polybenzimidazole peaks did not appear change as a result of UV irradiation; however, there is some uncertainty with this qualitative observation since these polybenzimidazole peaks were not well resolved and the oxidized species are similar to those for the polyaramids.

3.5. Impact of exposure on in-service turnout gear

The conversion of d on the SPHERE to d of NC and d of TGC were discussed in the "Experimental: UV Aging" section of this manuscript and the values are provided in Table 2. At 13 d on the SPHERE, the mechanical property deterioration had reached a steady to semi-steady state (Tables 3–6). The amount of simulated sunshine UV radiation at 13 d on the SPHERE is equivalent to the amount of natural sunshine (solar) UV radiation that turnout gear will be exposed to during 6.3 y of service assuming a daily exposure duration of 1 h.

Based on the data collected in this study the impact of UV exposure on turnout gear is as follows.

- UV radiation will significantly decrease the service life of OS constructed of NKB and KPB fabrics.

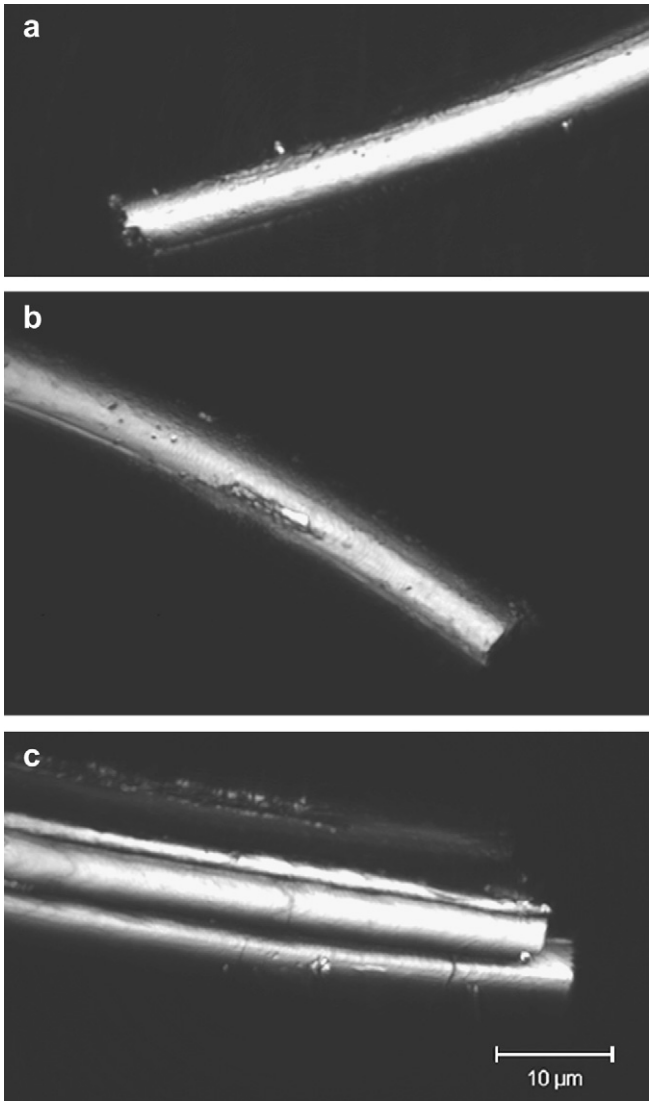

Fig. 14. Confocal microscope images of polybenzimidazole fiber fracture ends following tensile failure. These fibers were from KPB fabric following (a) 0 d, (b) 14 d, and (c) 56.6 d of UV irradiation at 50 °C and 50% RH. The fibers ends did not change as drastically as observed for the polyaramid fibers suggesting that polybenzimidazole and therefore its properties were less impacted by the UV radiation.

- ○ At 1.9 y of service, a NKB based OS lost 73% and 6 of its tear strength and tensile strength, respectively. In comparison, the KPB based OS fared better with a calculated loss of 40% and 22% of its tear strength and tensile strength, respectively.
- ○ At 6.3 y of service (the point at which further exposure has little impact on the property deterioration), a NKB based OS lost 83% and 89% of its tear strength of its tensile strength, respectively. In comparison, the KPB based OS fared better with a loss of 70% and 51% deterioration of the tear and tensile strength, respectively.
- ○ Surprisingly, our sensory observations did not indicate the performance of these OS fabrics had deteriorated. More specifically, when we pulled these OS fabrics using our hands they did not respond (qualitatively) any differently than the unexposed fabrics. In addition, these fabrics were only slightly darker in color.
- ○ Since sensory observations are the primary bases the fire community uses to initiate a request for gear replacement or repair, there is a strong possibility that turnout gear may be used with OS that are not providing adequate protection.

- UV radiation will degrade the water repellant coating.
  - ○ At 6.3 y of service, the NKB coating was gone and significantly degraded on the KPB fabric (based on ATR-FTIR analysis).
  - ○ The water absorption performance was not measured; therefore we cannot comment as to the impact of the degraded coating on this performance.
- Results indicated polybenzimidazole fibers were less impacted by UV radiation.
  - ○ The deterioration of mechanical properties of KPB fabrics may be less severe because the polybenzimidazole fibers appear to be more resistant to the UV radiation. In the future, we will measure the contribution of fabric construction (plain versus rip-stop weave) on the UV radiation induced deterioration of mechanical properties.
- As long as the undergarments (MB and TL) of turnout gear are covered by the OS, the undergarments are not exposed to UV radiation.

Table 9
FTIR Band Assignment for poly(*m*-phenylene isophthalate) based on Villar-Rodil et al. [22].

Band (cm^{-1})	Assignment
3300	N–H stretching in a trans amide
3065	C–H stretching vibrations in an unsaturated compound
1660	Amide I (amide C = 0)
1608	Aromatic ring C=C
1536	Amide II (N–H deformation and C–N stretching coupled modes)
1305	Aromatic C–N stretching
1240	Amide III
781, 685	Out-of-plane C–H vibration of meta-substituted ring
720	Amide V

Table 10
FTIR Band Assignment for poly(*p*-phenylene terephthalamide) based on Mosquera et al. [28].

Band (cm^{-1})	Assignment
3320	N–H stretching in a trans amide
3054	C–H stretching vibrations in an unsaturated compound
1646	Amide I (amide C = 0)
1608/1515	Aromatic ring C=C
1534	Amide II (N–H deformation and C–N stretching coupled modes)
1018	Out-of-plane C–H vibration of para-substitute aromatic rings

Table 11
FTIR Band Assignment for polybenzimidazole based on Chang et al. [23].

Band (cm^{-1})	Assignment
3402	"Free" N–H stretching
3145	"Associated" N–H stretching
3050	Aromatic N–H
1626	C=C/C=N stretching
1590	Benzene-Imidazole ring junction vibration
1528	In-plane ring vibration of 2-substituted benzimidazole
1423	In-plane ring vibration of 2,6-disubstituted benzimidazole
1401	C–C stretching
1287	Imidazole ring
1222	In-plane C–H deformation of 2,6-disubstituted ring
1017	Benzene ring vibration
984	Benzene ring vibration
955	In-plane C–H deformation of single H in benzene ring
902	C–H out-of-plane bending of a single H on benzene ring
852	C–H out-of-plane bending of 2 adjacent H on benzene ring
802	Heterocyclic-ring vibration or C–H out of plane bending of 3 adjacent H on benzene ring
705	Heterocyclic ring vibration

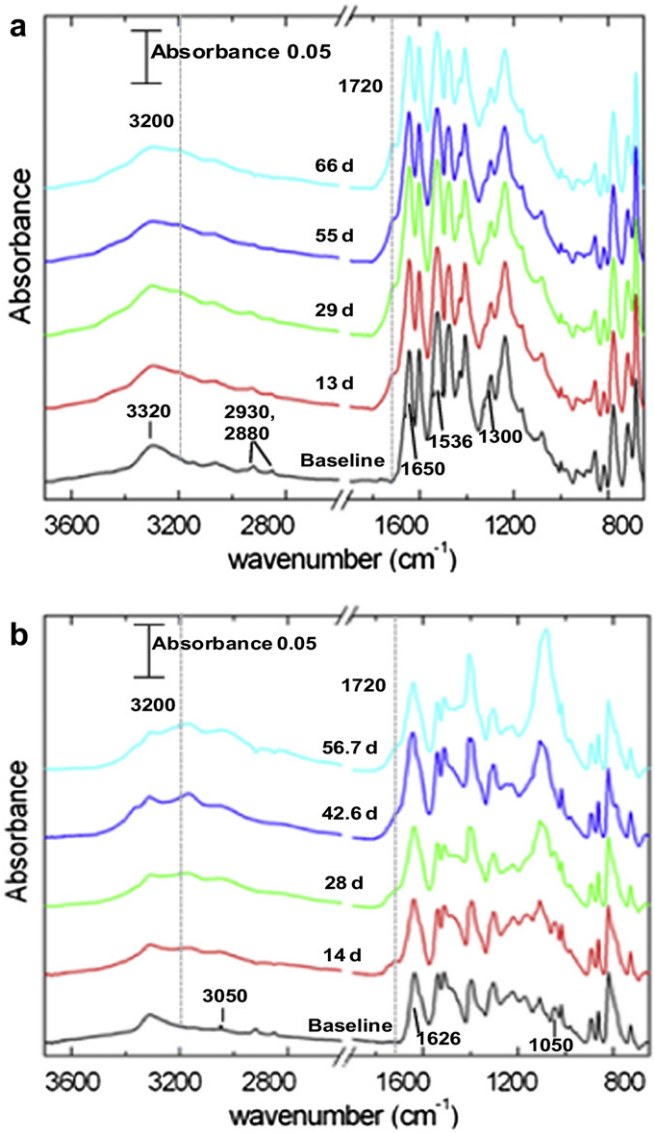

Fig. 15. ATR-FTIR spectra of (a) NKB and (b) KPB fabrics as a function of UV irradiation. Degradation products are represented by dotted lines. Other peaks are polyaramid and water repellant coating (a), and the polybenzimidazole in (b). It was assumed the polyaramids were photo-oxidized because of the formation of the 1702 cm^{-1} and 3320 cm^{-1} peaks and the intensity reduction of the 1536 cm^{-1} and 1650 cm^{-1} peaks. Standard uncertainty was $\pm$ 1 cm^{-1} in wavenumber and $\pm$ 5% in absorbance.

- The UPF value for OS constructed of NKB and KPB fabrics will decrease 42% and 28%, respectively, after 6.3 y of service. However, even at a 42% lower UPF value, the OS constructed of a NKB fabric is still blocking 96% of the UV radiation. At 27 y of service the mechanical performance of the OS constructed of these fabrics decreased by >85%, yet the OS still blocked 94.5% of the UV radiation.
- Most turnout gear is replaced within 10 y of service at which point the OS will still block > 95% of the UV radiation; therefore, replacing the OS to improve the UV protection of the undergarments is not necessary.

4. Conclusions

The goal of this research was to determine the impact of simulate sunshine UV irradiation (under typical in-service conditions) on fabrics commonly used in OS of commercial turnout gear and determine to what extent the undergarment could be damaged from UV transmission through the OS.

Unexposed KPB and NKB fabrics have very similar fabric density, tensile strength, and tear resistance, but the NKB fabric had a higher percent elongation and UV protection. UV irradiation significantly impacted the mechanical properties of these fabrics. LSCM and ATR-FTIR analysis revealed the irradiation caused polymer decomposition, which is assumed to be the reason for the drop in mechanical performance. The irradiation had less of an impact on the KPB fabric as evidenced by KPB outperforming NKB in every analysis and test, except for UPF and percent elongation where the fabrics performed very similar to each other.

The results, observations and conclusions of this study support NFPA 1971 [10] and NFPA 1851 [11] guidelines to not store turnout gear in direct sunlight. The tensile strength and tear resistance of outer shells constructed from the NKB Plain weave fabric will deteriorate at most 45% after 177 d of service, at most 90% after 6.3 y of service, and at most 93% after 10 y of service. The KPB Rip-Stop weave OS will better maintain its performance with a deterioration of at most 70% at 6.3 y of service and at most 75% at 10 y of service. However, the performance deterioration is significant regardless of the fabric type; therefore, it is recommended that turnout gear be exposed to as little UV radiation as possible. Since these fabrics block at least 94% of the UV radiation, even after 20 y of service, the undergarments (MB and TL) are not at risk of UV irradiation providing the OS is between the UV source (sun, fluorescent lights, etc.) and the undergarment. If the undergarments are experiencing UV degradation, it is likely from the gear being turned inside, which is common practice, i.e., drying the gear or placing the gear over the boots for quicker deployment of gear.

5. Future research

There are a number of parameters currently under investigation, or planned for, in the near future. These include, but are not limited to, measuring the individual contribution of each environmental stress (no UV, lower temperature) on performance deterioration, measuring the impact other stresses (soot, soil, laundering) have on performance deterioration, measuring the impact stresses have on other turnout gear fabric compositions, measuring the thermal performance of the fabric as a function of stress type and duration, and evaluating new technologies to mitigate performance deterioration.

Acknowledgement

Appreciation is extended to Professor S. Lee at National Tsing Hua University in Taiwan for his discussion and guidance throughout this work and Debbie Stanley of NIST for her assistance on UV-transmittance measurements and specimen exposure in the NIST SPHERE.

References

[1] Reproduced by the permission of SPERIAN Protective Apparel, Ltd.
[2] Chin J, Forster A, Clerici C, Sung L, Oudina M, Rice K. Temperature and humidity aging of poly(*p*-phenylene-2,6-benzobisoxazole) fibers: Chemical and physical characterization. Polymer Degradation and Stability 2007;92(7):1234–46.
[3] Mera H, Takata T. High performance polymers. In: Ullmann's encyclopedia of industrial chemistry. Weinheim: Wiley-VCH; 2005.
[4] Polybenzimidazole - Goodfellow, online source, sources, small quantity, quantities [Internet]. [cited 2010 Feb 2]; Available from: http://www.goodfellow.com/E/Polybenzimidazole.HTML.
[5] Sugama T. Hydrothermal degradation of polybenzimidazole coating. Materials Letters 2004;58(7–8):1307–12.

[6] Zhang H, Zhang J, Chen J, Hao X, Wang S, Feng X, et al. Effects of solar UV irradiation on the tensile properties and structure of PPTA fiber. Polymer Degradation and Stability 2006;91(11):2761–7.
[7] Tincher W, Carter W, Gentry D. Protection of Nomex from Ultraviolet Degradation [Internet]. Georgia Technical Institute; 1977 [cited 2010 Feb 2]. Available from: http://www.dtic.mil/cgi-bin/GetTRDoc?AD=ADA041494&Location=U2&doc=GetTRDoc.pdf.
[8] ATL_309_Ci3000Bro_FNL_8_30.pdf [Internet]. [cited 2010 Feb 2]; Available from: http://www.atlas-mts.com/shopdownloads/23/ATL_309_Ci3000Bro_FNL_8_30.pdf?sessionid=f690c7285ad275079e38f8bef644b6c90.
[9] Chin J, Byrd E, Embree E, Martin J. Integrating sphere sources for UV exposure: a novel approach to the artificial UV weathering of coatings, plastics and composites. In: Service life prediction: methodologies and metrologies. p. 144–60. Available from: http://www.fire.nist.gov/bfrlpubs/build03/PDF/b03045.pdf; 2002.
[10] 1971 Standard on protective ensembles for structural fire fighting and proximity fire fighting. National Fire Protection Association; 2007.
[11] 1851 Standard on selection, care, and maintenance of protective ensembles for structural fire fighting and proximity fire fighting. National Fire Protection Association; 2008.
[12] Chin J, Embree E, Garver N, Dickens J, Finn B, Martin J. Accelerated UV weathering device based on integrating sphere technology. Review of Scientific Instruments 2005;75(11):4591–959.
[13] G173-03e1 Standard tables for reference solar spectral irradiances: direct normal and hemispherical on 37° Tilted Surface [Internet]. American Standard Test Methods. Available from: http://www.astm.org/Standards/G173.htm; 2005.
[14] D2261-96 Standard test method for tearing strength of fabrics by the tongue (single rip) procedure (constant-rate-of-extension tensile testing machine). American Standard Test Methods. Available from: http://www.astm.org/DATABASE.CART/HISTORICAL/D2261-96R02.htm; 2002.
[15] Textile warping is the process of creating the base yarn that runs top to bottom on woven cloth. In a basic two yarn woven fabric, the warp is the continuous row of yarns and the weft is the yarns woven in from side to side.
[16] Davis RD, Chin J, Lin CC, Petit S. Effect of accelerated ultraviolet weathering on firefighter protective clothing outer shell fabrics. National Institutes of Standards and Technology Technical Note 1657, in press.
[17] TM183-2000 transmittance or blocking of erythemally weighted ultraviolet radiation through fabrics. American Association of Textile Chemists and Colorist. Available from: http://www.dfmg.com.tw/member/standard/aatcc/aatcc/Front.pdf; 2008.
[18] Gorensek M, Sluga F. Modifying the UV blocking effect of polyester fabric. Textile Research Journal 2004;74(6):469–74.
[19] Roy CR, Gies HP. Protective measures against solar UV exposures. Radiation Protection Dosimetry 1997;72(3–4):231–40.
[20] D6603-00 Standard guide for labeling of UV-protective textiles [Internet]. American Standard Test Methods. Available from: http://www.astm.org/Standards/D6603.htm; 2003.
[21] Hearle JWS, Lomas B, Cooke W. Atlas of fiber fracture and damage to textiles. 2nd ed. Boca Raton, FL: CRC Press LLC. Available from: http://www.amazon.com/Atlas-Fracture-Damage-Textiles-Second/dp/0849338816#reader_0849338816; 1998 [cited 2010 Feb 2].
[22] Villar-Rodil S, Paredes JI, Martinez-Alonso A, Tascon JMD. Atomic force microscopy and infrared spectroscopy studies of the thermal degradation of Nomex Aramid fibers. Chemistry of Materials 2001;13(11):4297–304.
[23] Chang Z, Pu H, Wan D, Liu L, Yuan J, Yang Z. Chemical oxidative degradation of Polybenzimidazole in simulated environment of fuel cells. Polymer Degradation and Stability 2009;94(8):1206–12.
[24] Jang M, Yamazaki Y. Preparation, characterization and proton conductivity of membrane based on zirconium tricarboxybutylphosphonate and polybenzimidazole for fuel cells. Solid State Ionics 2004;167:107–22.
[25] Coates J. Interpretation of infrared spectra, a practical approach. In: Encyclopedia of analytical chemistry. Chinchester: John Wiley and Sons Ltd.; 2000. p. 10815–37.
[26] Tiefenthaler AM, Urban MW. Surface studies of polymer films and fibers by CIRCLE ATR FT-IR. Applied Spectroscopy 1988;42:163–6.
[27] Deimede V, Voyiatzis GA, Kallitsis JK, Qingfeng L, Bjerrum NJ. Miscibility behavior of polybenzimidazole/sulfonated polysulfone blends for use in fuel cell applications. Macromolecules 2000;33(20):7609–17.
[28] Mosquera MEG, Jamond M, Martinez-Alonso A, Tascon JMD. Thermal transformations of Kevlar Aramid fibers during pyrolysis: infrared and thermal analysis studies. Chemistry of Materials 1994;6(11):1918–24.
[29] Luo J, Sun Y. Acyclic N-Halamine coated Kevlar fabric materials: preparation and biocidal functions. Industrial & Engineering Chemistry Research 2008;47(15):5291–7.